

GROUND MAGNETIC CHARACTERISTICS OF SOLAR DIURNAL VARIATIONS: PRELIMINARY RESULTS.

Klausner V.^{1,2}, *Mendes O.*³, *Papa A. R. R.*^{4,5}, and *Domingues M. O.*⁶

¹ Observatório Nacional, Rio de Janeiro, Brazil, virginia@on.br

² Instituto Nacional de Pesquisas Espaciais, São José dos Campos, Brazil, virginia@dge.inpe.br

³ Instituto Nacional de Pesquisas Espaciais, São José dos Campos, Brazil, odim@dge.inpe.br

⁴ Observatório Nacional, Rio de Janeiro, Brazil, papa@on.br

⁵ Universidade do Estado do Rio de Janeiro, Rio de Janeiro, Brazil, papa@uerj.br

⁶ Instituto Nacional de Pesquisas Espaciais, São José dos Campos, Brazil, margarete@lac.inpe.br

Abstract: Using hourly magnetogram dataset, we explore the solar diurnal variations via a time-scaled gapped wavelet analysis. This work aims mainly to highlight and interpret these diurnal variations over Southeast Brazil. A comparison of them to features from other magnetic stations distributed over the whole Earth's surface is also done.

Keywords: Gapped Wavelet Analysis, Magnetogram data, Diurnal Variations.

1. INTRODUCTION

The first reports of a regular quiet-day variation of the geomagnetic field dated from 1634 in London [1]. In 1882, Thompson (later known as Lord Kelvin), in a presidential address to the Royal Society of Edinburg, discussed the harmonic components of the solar daily variations saying the cause of the semi-diurnal variation couldn't be generated by gravitational-tide but variation of temperature due to the effects of Earth's rotation [2]. These thermotidal forces cause ions to move through Earth's magnetic field and thus generate ionospheric currents. The E-region of the ionosphere permits the flow of these electron currents between 90 and 130 km due to the ion density and the collision frequency, called the Sq currents (S=solar, q=quiet). The dynamo currents of Sq form two whorls on the dayside of the Earth clockwise in the North Hemisphere and anticlockwise direction in the South Hemisphere. At the magnetic dip equator, the geomagnetic field is horizontally directed from South to North. This special condition increases considerably the East-West ionospheric conductivity allowing an intense eastward current to flow, called the "equatorial eletrojet" [3].

The prevalent harmonics in the analysis of the quiet-day time series are: 24-, 12-, 8- and 6-hours period [4]. Diurnal is always used to mean a harmonic variation with period of one day. Semidiurnal, terdiurnal and quaterdiurnal represent respectively the periods of 12, 8 and 6 hrs. To study the harmonics of the solar diurnal variations, we used the hour data of the H component and we explored it via a time-frequency gapped wavelet algorithm. Standard wavelet

methods require times series to be regularly distributed in time. So, the gapped wavelet technique is suitable for analysis of data with gaps, especially in our case, using data from various magnetic stations that present gaps in the records in different periods of time. This work aims mainly to highlight and interpret the solar diurnal variations over the Brazilian sector compared to the features from other twelve magnetic stations reasonably distributed over the whole Earth's surface. By applying wavelet transforms to these signals, we are able to analyze both the frequency content of each signal and the time dependence of that content. After computing wavelet transforms of the data, we perform wavelet cross-correlation analysis. The wavelet cross-correlation technique is useful to isolate the period of the spectral components of geomagnetic field in each station and to correlate them as function of scale (period).

Although wavelet transforms were originally applied in geophysics to analyze seismic signals [5], today the wavelet techniques have exponentially grow in many different areas. The same thing is happening with the wavelet cross correlation. In physiological research, Oczeretko and his colleagues [6] used the wavelet cross-correlation method to assess the synchronization between contractions in different topographic regions of the uterus, as a potential diagnostic alternative in various pathologies.

Rehman and Siddiqi [7] researched correlations between pairs of time series of meteorological parameters such as pressure, temperature, rainfall, relative humidity and wind speed to study the climatic dynamics in different location using wavelet cross-correlation.

Frick and other researchers [8] analyzed nine optical and radio maps of a nearby spiral galaxy NGC 6946 using correlation between images as function of scale. In space weather research, the wavelet correlation was first introduced by [9] to study two time series of solar data.

Section 2 is devoted to present a brief of continuous wavelet transform. Section 3 is devoted to introduce the gapped wavelet analysis. In Section 4, we introduce the wavelet cross-correlations and discuss how they can be quantified. In Section 5, the data and the analyzed period are presented. In Section 6, a discussion about the results is

given. Finally, in section 7 follows the conclusion of this work.

2. CONTINUOUS WAVELET TRANSFORM (CWT)

The *wavelet transform* was introduced at the beginning of the 1980s by *Morlet and Grossman*, who used it to evaluate seismic data [5]. They modified the Gabor transform, also known as Windowed Fourier Transform, to produce the continuous wavelet transform. The idea was to change the width of the window function accordingly to the frequency of the signal being considered. The CWT, also called the *integral wavelet transform (IWT)*, finds most of its applications in data analysis, where it yields an affine invariant time-frequency representation.

In order to a function be called *wavelet* it must satisfy the following conditions:

1) The area under the curve described by the function ψ , must be zero

$$\int_{-\infty}^{\infty} \psi(t) dt = 0 \quad (1)$$

This condition is known as the admissibility condition and assures that the wavelet have a mean zero.

2) The energy must be unitary

$$\int_{-\infty}^{\infty} |\psi(t)|^2 dt = 1 \quad (2)$$

The second condition assures that the function is localized in both, physical and Fourier, spaces (time and frequency), i.e., the Heisenberg relation $\Delta t \Delta \omega = \text{const}$ must be satisfied.

The CWT of a time series f is defined by the integral transform,

$$W(a, b) = \int f(t) \psi_{a,b}^*(t) dt \quad (3)$$

This function represents a one-dimensional signal as a function of both time and frequency (position (b) and scale (a)) and is similar to a local, filtered Fourier transform that can be obtained by dilating and translating the wavelet (ψ) and convolving it with the signal (f). The function ψ is called the mother-wavelet function and expressed as

$$\psi_{a,b}(t) = \frac{1}{\sqrt{a}} \psi\left(\frac{t-b}{a}\right), \quad a > 0 \quad (4)$$

The pre-factor $|a|^{1/2}$ is introduced in order to ensure that all the scaled functions $|a|^{1/2} \psi(t/a)$, with $a \in \mathfrak{R}$, have the same energy. The parameter b simply means a translation in time of a wavelet with fixed a convolving with the signal (f). However, the time-frequency resolution of the wavelet transform depends on scale a . For high frequencies analysis (small a) we have good time localization but poor frequency resolution. On the other hand, for low frequencies analysis, we have good frequency resolution but poor time localization.

The choice of the wavelet function depends on both: data and analysis goals. In this work, our purpose is to preserve the time-frequency balance. Also, the characteristic of the wavelet transform depends on the chosen mother wavelet. For example, to represent a time series with abrupt variations or steps, the Haar wavelet may be the most

convenient, but for smoother time series, Morlet and Maar wavelet are more recommended.

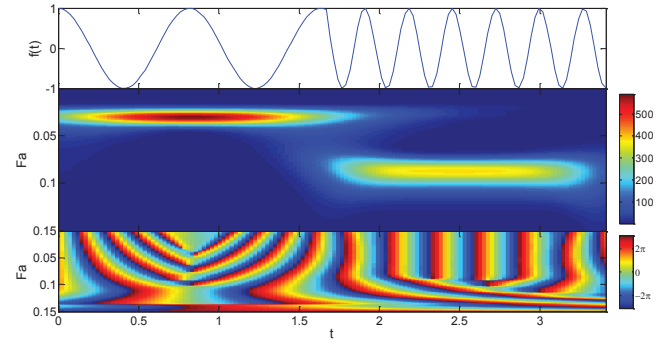


Fig. 1. Spectrogram of an artificial sinusoidal signal consisting of 30 mHz and 90 mHz. (a) sample of a sinusoidal waveform; (b) continuous wavelet spectrogram which satisfactorily resolves both in time and frequency; (c) phase changes of the data.

It is possible to analyze a signal in a time-scale plane, the wavelet spectrogram, which is also called, wavelet scalogram. In analogy with the Fourier analysis, the square modulus of the wavelet coefficient is used to provide the energy distribution in the time-scale plane. Figure 1(a) shows a sample waveform, in which the frequency changes in time. As shown in Fig. 1(b), the wavelet decomposition with the complex Morlet wavelet can reproduce the frequency changes in Fig. 1(a), which indicates that the wavelet analysis is useful for multi-scale phenomena. Also, the phase changes can be analyzed as shown in Fig 1 (c), which allows us to retrieve the oscillatory behavior on the data.

3. GAPPED WAVELET ANALYSIS

Magnetogram Data is a finite length observational data series and may contain gaps of various sizes. To reduce gap problems, we use the gapped wavelet analysis — a technique introduced by Frick and colleagues [10] and developed in [11]. In this transform, the admissibility condition is broken when the wavelet overlaps the data gaps. The leading idea of the gapped technique is to restore the admissibility condition by repairing in some way the wavelet itself.

Following [10], we separate the analyzing wavelet in two parts, the oscillatory part $h(t)$ and the envelope $\phi(t)$,

$$\psi = h(t) \phi(t) \quad (5)$$

$$h(t) = \exp(i\omega_0 t) \quad (6)$$

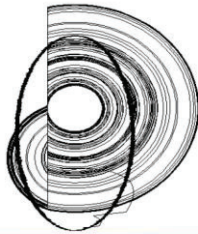
$$\phi(t) = \exp(-t^2/2) \quad (7)$$

In the case when the wavelet is disturbed by the gap, we can restore the admissibility condition by including a parameter C in the oscillatory part of the wavelet,

$$\tilde{\psi}(t, b, a) = \left[h\left(\frac{t-b}{a}\right) - C(a, b) \right] \phi\left(\frac{t-b}{a}\right) \quad (8)$$

and requiring,

$$\int_{-\infty}^{\infty} \tilde{\psi}(t) dt = 0 \quad (9)$$



DINCON'10

9th Brazilian Conference on Dynamics,
Control and their Applications
June 07-11, 2010



The introduced parameter C can be determined for each scale a and position b from (8) and (9).

$$C(a, b) = \left[\int_{-\infty}^{\infty} \phi\left(\frac{t-b}{a}\right) dt \right]^{-1} \left[\int_{-\infty}^{\infty} h\left(\frac{t-b}{a}\right) \phi\left(\frac{t-b}{a}\right) dt \right] \quad (10)$$

The mathematical properties of this algorithm were studied in detail by Frick et al. [11]. It was shown that this technique not only suppresses the noise, caused by the gaps and boundaries, but improves the accuracy of frequency determination of short or strongly gapped signals.

4. METHOD OF ANALYSIS: THE WAVELET CROSS-CORRELATION.

In this paper, we used the Morlet wavelet,

$$\psi(t) = e^{-t^2/2} e^{i\omega_0 t} \quad (11)$$

with $\omega_0 = 6$.

The Morlet mother wavelet is suited very well for experimental data analysis because it has a Gaussian envelope. It allows reach a reasonable compromise between the time-frequency resolutions.

The approach of this work is to use the wavelet cross-correlation to study the correlation between a pair of magnetic data from different stations as a function of scale:

$$C(a) = \frac{\int W_1(a, t) W_2(a, t) dt}{\left(\int W_1^2(a, t) dt \int W_2^2(a, t) dt \right)^{1/2}} \quad (12)$$

where $W_i(a, t) = |w_i(a, t)| - \overline{|w_i(a, t)|}$ and w_i are the wavelet coefficients and $\overline{w_i}$ is the arithmetic mean.

We can obtain also the coefficient of determination as function of the scale. It is calculated by (and defined as) the square of the correlation coefficient, and gives the proportion of variance between the data.

As we mention above, in the wavelet representation the scale (a) defines the distribution of energy of the whole signal through time. The wavelet cross-correlation allows us to check the interaction between two sets of data for each considerate scale. The scales are chosen in a way that makes possible to characterize the dominating periods present in the geomagnetic data spectrum.

5. DATASET.

In this paper, we used ground magnetic measurements to study the correlation between Vassouras (VSS - RJ, Brazil) and other 12 different magnetic stations, which we selected to provide a reasonably homogeneous distribution of the measurements on the Earth's surface. The distribution of the magnetic stations, with their IAGA code, is given in Figure 2 and the correspondent code and location in Table 1. This work relies on data collections provided by the INTERMAGNET programme (<http://www.intermagnet.org>).

We choose the period of one month to analyze, March, 2005 that corresponds to a low solar activity year. This period presents quiet and disturbed days. By checking the solar geophysical index series (Dst - Disturbance Storm Time) from the World Data Center in Kyoto, this month present high Dst index of -65 on the sixth day.

We used low- and mid-latitude magnetic station so the magnetograms for these days should be not serious affected by these magnetic disturbances and the Sq would correspond to a regularly recurring phenomena each day in these stations.

Table 1. INTERMAGNET network of geomagnetic stations used in this study.

ABB CODE	GEO LAT	GEO LONG	GEOMAG LAT
AMS	-37.80	77.57	-46.40
ASP	-23.76	133.88	-32.91
BEL	51.84	20.79	50.23
BMT	40.30	116.20	30.13
BOU	40.13	-105.23	48.40
CLF	48.03	2.26	49.84
CMO	64.87	-147.86	65.38
EYR	-43.41	172.35	-47.11
HER	-34.35	19.25	-33.97
HON	21.32	-158.00	21.64
KAK	36.13	140.11	49.32
SJG	18.11	-66.15	28.58
VSS	-22.40	-43.65	-13.29

Source: <http://swdewww.kugi.kyoto-u.ac.jp/wdc/obsdata.html> (2010).

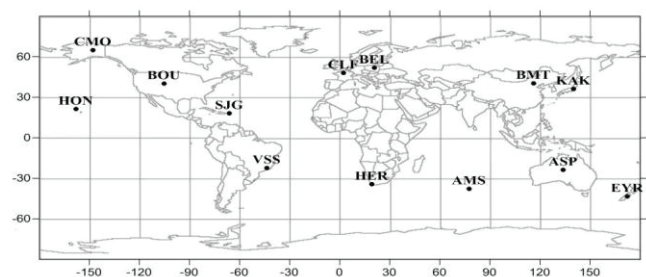


Fig. 2. The localization of the stations and their respective IAGA code.

By international agreement, the Earth's field components are described by the "right-hand system". It means that the x direction would be indicated by our thumb, the y direction by our pointing finger and the z direction by the remaining fingers. However, the Earth's field can be described in two

ways: (1) three orthogonal component field called the X , Y and Z representation or (2) the horizontal magnitude, the eastward angular direction of the horizontal component from geographic northward and the downward component called, respectively, the H (horizontal), D (declination) and Z (vertical) representation. Figure 3 illustrates these nomenclatures for a location in the Northern Hemisphere where the total field vector points into the Earth [3].

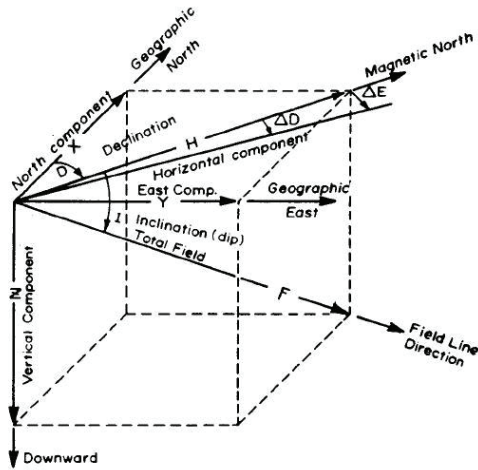


Fig. 3: Components of the geomagnetic field measurements. Source: Campbell, 1997.

In this work, we focus to study geomagnetic variations well-known as solar diurnal variations, in particularly the diurnal and semidiurnal tide. These features were greatly explored over the decades, as well its spatial dependence primary on latitude and others factors including time of year and level of solar activity [3, 4, 12, 13, 14, 15, 16 and 17]. We took in consideration the two well-known fact about the Sq field: 1) is largely a local time field that can be roughly represented by a current fixed to the Sun, so we used the data at Universal Time (UT) and that the is a content of pattern by the Earth's main field throughout the latitudes between 60°N and 60°S , so we didn't used magnetic stations of high latitudes (auroral zone). At high latitudes, the ionospheric currents are joined with the field-aligned currents (FAC) from solar wind region into the magnetosphere, and the electrodynamic is dominated by the influences of the solar-wind-magnetosphere interaction processes. On the other hand, the ionospheric current at middle and low latitude is generated by ionospheric wind dynamo.

Our primary interest is to correlate the response of the geomagnetic field at Vassouras to the other twelve previously chosen magnetic stations. The Vassouras Magnetic Observatory, Rio de Janeiro, Brazil, has been active since 1915 and is a member of the INTERMAGNET programme. One of the peculiarities of VSS is its location, low latitude, where the H component is essentially the same as the total geomagnetic field. In the next years, a Brazilian network of magnetometers will be implemented and VSS can be used as reference.

To fulfill our purpose, we used hourly mean value series of the H geomagnetic component. Some magnetic stations have available solely the X component, so we converted the X component of XYZ system to the H component of the HDZ

system of vector representation of the Earth's magnetic field,

$$X = H \cos(D) \quad (13)$$

where X is the vertical component in the XYZ system, H is the horizontal magnitude and D (declination) is the angular direction of the horizontal component from the geographic north (see Figure 3). This conversion of system was possible because we used magnetic stations of low- and mid latitudes.

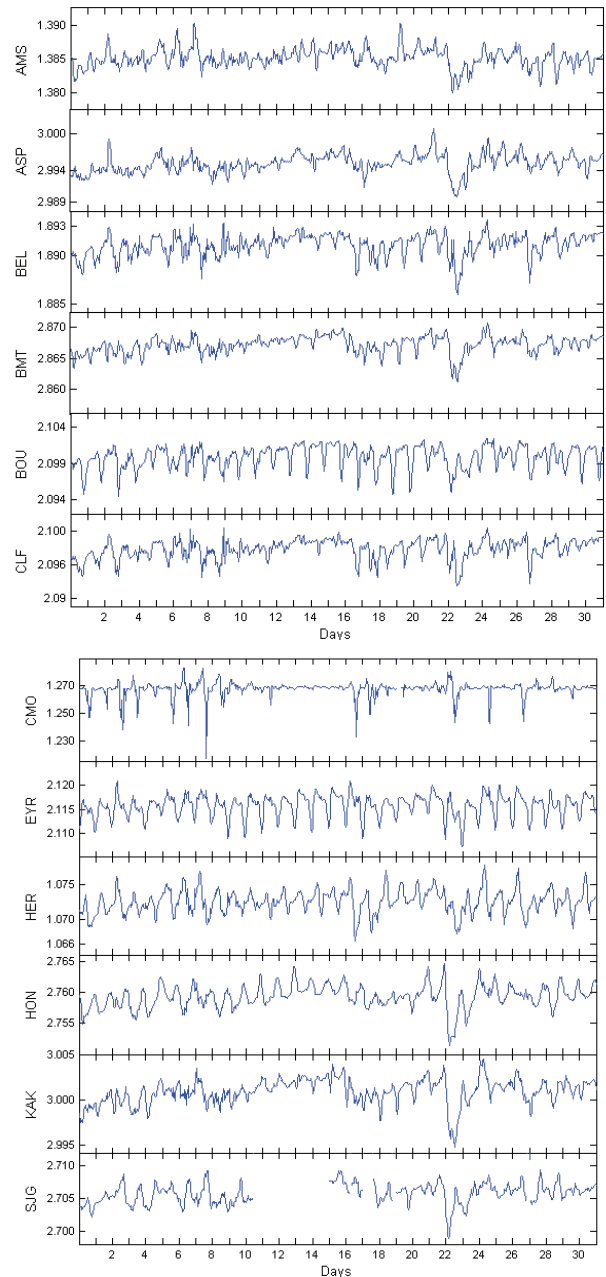
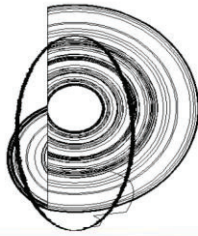


Figure 4. Dataset to characterize the magnetic variations for March 2005. Each painel shows from top to bottom the X or H -component of the geomagnetic field for the stations: AMS, ASP, BEL, BMT, BOU, CLF, CMO, EYR, HER, HON, KAK and SJC.

Figure 4 shows the behavior of the X or H -component of the Earth's geomagnetic field. We can observe a magnetic signature of 12 chosen magnetic stations used in this work to calculate the wavelet cross-correlations. The stations of



AMS, ASP, BEL and CLF have available solely the X component that it was afterward converted to H component for the wavelet analysis. In Figure 4, each panel shows, from top to bottom, the stations: AMS, ASP, BEL, BMT, BOU, CLF, CMO, EYR, HER, HON, KAK and SJG. It's possible to observe a presence of gaps on the datasets of CMO and SJG.

An adequate knowledge of the daily variation field and full understand of the associated phenomena, can only come from extensive and detailed analysis of the mean hourly values of the magnetic elements at many stations. So, the availability of these data in the World Data Centers that collect and distribute these data is of enormous help for researches like us.

5. RESULTS AND DISCUSSION

We started by calculating the wavelet coefficients for each chosen station using the Morlet wavelet. Also, we treat the gaps using the technique introduced by [10] as we discussed in session 3.

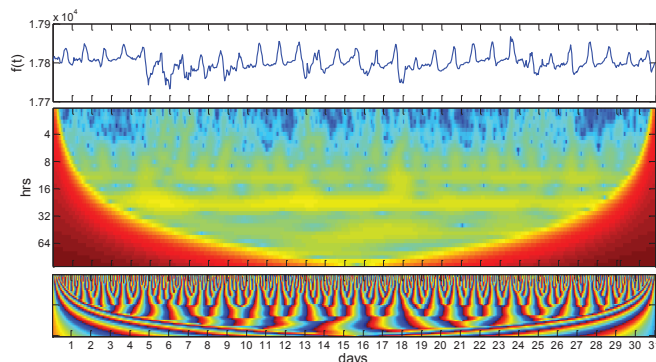


Fig. 5. Each panel shows from top to bottom H component time series of VSS Station at March, 2005 used for the wavelet analysis, the local wavelet power spectrum using the Morlet wavelet and the phases changes of the dataset.

A Morlet wavelet power spectrum analysis of the H component for March, 2005 of Vassouras station is shown in Figure 5. Areas of stronger wavelet power are shown as yellow color on a plot of time horizontally and time scale vertically. The wavelet power at times underneath the cone of influence is not reliable. We are able to determine both the dominant modes of variability and how those modes vary in time. In the wavelet spectrum, it is clearly visible the 24 hrs and less dominant the 12 hrs period. The phase changes allow us to retrieve the oscillatory behavior on the data. With these wavelet coefficients, we calculated 12 cross-correlation functions $C(a)$, one for each pair of Vassouras and one of the 12 chosen magnetic stations. They are shown in Figure 6, where the graphs are displayed from top to bottom, in exactly the same order as in Table 1. These selected stations are divided in low latitude (ASP, BMT, HER, HON, KAK and SJG), medium latitude (AMS, BEL, BOU, CLF and EYR) and high latitude (CMO). For

convenience of visual inspection and comparison, the periods of 24, 12, 8 and 6 hrs are highlighted in Figure 6.

Figure 6 shows that for most of the pairs $C(a)$ varies considerably with scale. We observe that the correlation between two geomagnetic data sets, from different stations, is scale dependent. They are strongly correlated or less correlated depending on the scale.

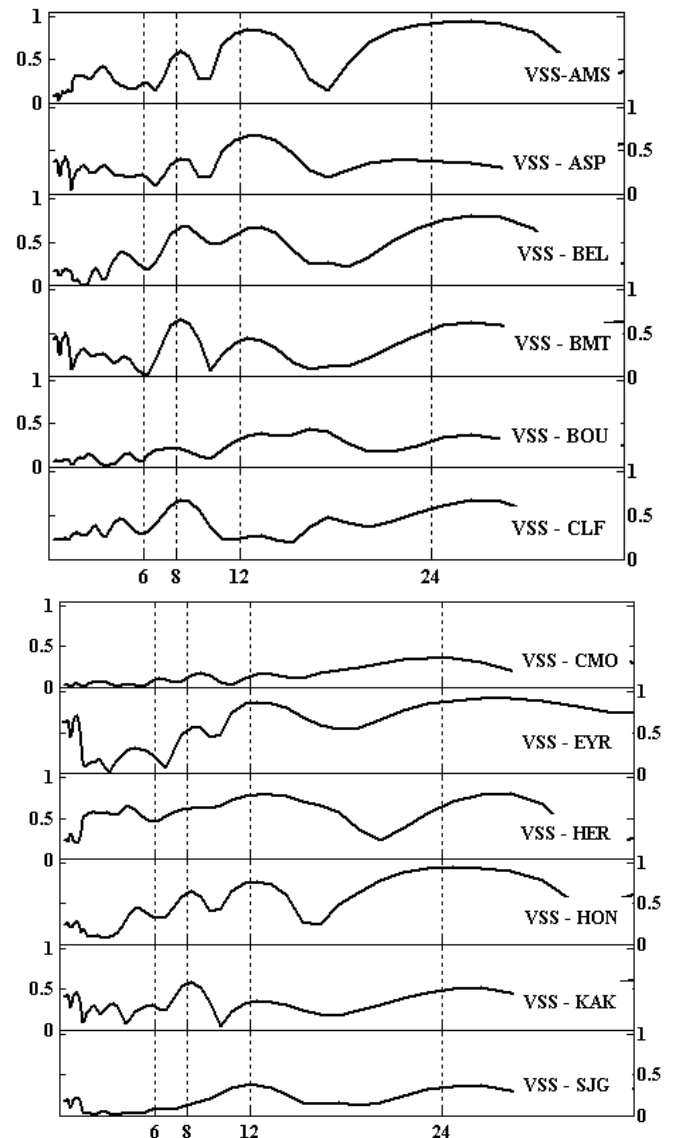


Fig. 6. Wavelet cross-correlation for the Vassouras and the 12 chosen magnetic stations.

As shown in Table 2, the wavelet cross-correlation between VSS and HON presents the best coefficient of determination explaining 88% of the time series variance for the solar diurnal variations (24 hrs period). Also AMS and EYR present a coefficient of determination above 75%. The less correlated cases (less than 50%) for the 24 hrs period

were the stations of ASP, BMT, BOU, CLF, CMO, HER, KAK and SJG.

Table 2. The coefficient of determination estimated using the wavelet cross-correlation function between Vassouras and the other 12 stations as a function of scale (period of 24 and 12 hrs).

CODE	24 hrs	12 hrs
AMS	0.87	0.70
ASP	0.14	0.44
BEL	0.56	0.42
BMT	0.34	0.19
BOU	0.11	0.13
CLF	0.37	0.07
CMO	0.13	0.02
EYR	0.79	0.75
HER	0.49	0.62
HON	0.88	0.59
KAK	0.25	0.12
SJG	0.13	0.14

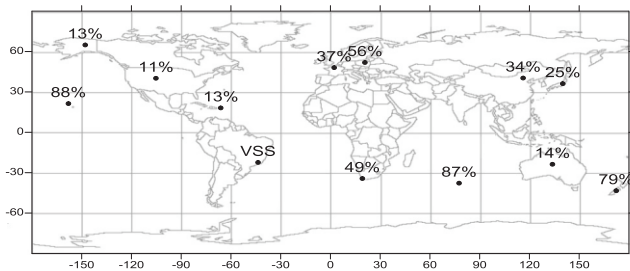


Fig. 7. The spatial pattern of coefficient of determination of the geomagnetic diurnal variation (24 hrs period) at the twelve chosen stations.

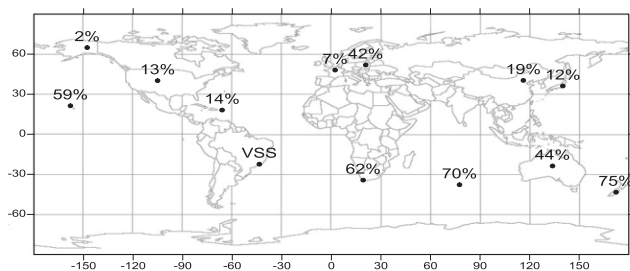


Fig. 8. The spatial pattern of coefficient of determination of the geomagnetic semidiurnal variation (12 hrs period) at the twelve chosen stations.

Figure 7 and 8 shows the spatial pattern of the coefficient of determination estimated using wavelet cross-correlation between VSS and the other twelve chosen magnetic stations for the diurnal and semidiurnal tides, respectively. The values of the coefficient of determination for each respectively stations are shown in Table 2. The maps shown in Figure 7 and 8 give a better idea of the latitudinal and longitudinal of the spatial relation between

the magnetic stations. These Figures suggest a longitudinal dependence over a latitudinal dependence, especially for the diurnal variation.

So, we found that the 24-h diurnal tide presented differences in the coefficient of determination for magnetic stations located in approximately the same geomagnetic latitude but different longitudes, this mean that these stations are affected differently by the dynamo. The asymmetry in the geomagnetic field produces the longitudinal dependence in the dynamo system through the following interrelated characteristics: inter-hemispheric coupling (field aligned currents), modulation of the dynamo's electromotive forces and conductivities and the asymmetric feedback on neutral wind dynamics [12, 13]. Also, the Sq current system is not symmetrical about the dip equator or any equator, even during equinoctial months and also, it is slight more intense during equinoctial months.

The total geomagnetic field is particularly high in regions of central of Canada, Siberia and south of Australia and it's quite low near southern Brazil. In addition, the dynamo-generating E region of the ionosphere is just about 100 km from the Earth's surface; in this short distance the local strength and direction determine the conductive character [3].

It is possible to observe that the magnetic stations located at the northwest of Canada (CMO) and Australia (ASP) presented lower coefficient of correlation if compared to other stations, as [3] affirmed. Also, the Sq1 model of Campbell and his colleagues [3], which is built from a spherical analysis similar to that of Matsushita and Maeda in 1965 (e.g. [3]), has shown differences in the longitudinal behavior of the *H* component between the American sector and the Africa and Asia sectors. During the equinox at the same dip latitude, the *H* component in the Asia and Africa sector had a very similar behavior characterized by a positive peak around noon, while in the American sector this peak is negative and accompanied by a positive secondary peak in the morning.

For the semidiurnal cycle, the stations of AMS and EYR present coefficients of determination above 70% while the stations of ASP, BEL, BMT, BOU, CLF, CMO, KAK and SJG, under 50%. The semidiurnal oscillation is much more irregular than the diurnal oscillation. Also, the semidiurnal oscillation presents a more defined latitudinal dependence. Both terdiurnal and quaterdiurnal oscillations present very irregular coefficients of correlation.

We expect lower correlation between VSS and CMO, because CMO is the station located at the higher latitude. At high latitudes a large horizontal current flows in the D and E regions of the auroral ionosphere that is called the Auroral Electrojet. There are two main factors in the production of the electrojet. First of all, the conductivity of the auroral ionosphere is generally larger than that at lower latitudes. Secondly, the horizontal electric field in the auroral ionosphere is also larger than that at lower latitudes. Since the strength of the current flow is directly proportional to the vector product of the conductivity and the horizontal electric field, the auroral electrojet currents are generally larger if compared to those at lower latitudes. During disturbed periods, these currents are intensified and their limits can



DINCON'10

9th Brazilian Conference on Dynamics,
Control and their Applications
June 07-11, 2010



extend beyond the auroral region. This expansion is mostly caused by enhanced particle precipitation and enhanced ionospheric electric fields [14].

Also, the oceans, as well as the ionosphere, constitute electrical conductors and are subject to tidal motions so we might expect some kind of dynamo to operate through tidal flow of ocean water [15]. So, observatories on islands or coastlines are fully exposed to anomalous effects of the ocean [16, 17]. The oceanic tides can induce an electric current system due to the drifting motion that produces some magnetic daily variation in magnetic stations on oceanic islands and nearby shores. This shows that care must be taken when interpreting the solar magnetic variations at a particularly station, if the purpose is to obtain a world-wide analysis of the Sq field. Though the ionosphere current may have a fairly simple world-wide pattern and the average induced current a similar pattern, the relatively small pattern of the conductivity of the surface layers of the earth will introduce a corresponding small scale pattern into the distribution of the induced currents. So, at certain stations, the solar magnetic variations may not give an accurate indication of the average induced current system [18].

As we used both quiet and disturbed days, the additional variations of the wavelet cross-correlation are related to the effect of equatorwards penetration of electric fields from the field-aligned current [19], ground conductivities, differences of the intensity of the geomagnetic field, effect of the ocean and ionospheric conductivities.

3. CONCLUSION

A world-wide distribution of the harmonic component of a solar diurnal variation has been observed in latitude and longitude in relation to the VSS station by using the gapped wavelet analysis and the wavelet cross-correlation technique.

The main remarks in this analysis can be summarized as follows:

1. The gapped wavelet analysis is an alternative technique to study a finite length observational data series that contain gaps of various sizes.

2. The wavelet cross-correlation technique is useful to isolate the period of the spectral components of the geomagnetic field in each station and to correlate them as function of scale (period).

3. The wavelet cross-correlation between VSS and HON presents the best coefficient of determination explaining 88% of the time series variance for the solar diurnal variations (24 hrs period). Also AMS and EYR present a coefficient of determination above 75%. The less correlated cases (less than 50%) for the 24 hrs period were the stations of ASP, BMT, BOU, CLF, CMO, HER, KAK and SJG.

4. For the semidiurnal cycle, the stations of AMS and EYR present coefficients of determination above 70% while

the stations of ASP, BEL, BMT, BOU, CLF, CMO, KAK and SJG, under 50%.

5. AMS and EYR were the magnetic stations that presented the most correlated responses of the diurnal and semi-diurnal to VSS station.

6. The terdiurnal and quaterdiurnal oscillations were very irregular.

7. Some peculiarities of the coefficient of determination between the magnetic stations are related to the effect of equatorwards penetration of electric fields from the field-aligned current, ground conductivities, differences of the intensity of the geomagnetic field, effect of the ocean and ionospheric conductivities.

These results suggest that such characteristics of solar diurnal variations over the Brazilian sector compared to the features from other magnetic stations are important to understand the dynamics of horizontal-field variations involved in the monitoring of the Earth's magnetic field. And we are particularly focused in understanding the response of the Vassouras Observatory (VSS), because in the next years, a Brazilian network of magnetometers will be implemented and VSS will probably be used as a reference.

ACKNOWLEDGMENTS

V. Klausner wishes to thank CAPES for the financial support of her PhD. Also, the authors would like to thank CAPES/PAEP (proc. number: 0880/08-6), CNPq (proc numbers: 486165/2006-0, 308680/2007-3 and 309017/2007-6) and FAPESP (proc number: 2007/07723-7), and INTERMAGNET programme for the datasets used in this work.

REFERENCES

- [1] Von Humboldt, A., "Cosmos", Vol V (English translation by E. C. Otté and W. S. Dallas). Harper and Bros Pub., New York, 1863.
- [2] Thompson (later Lord Kelvin), "On the Thermodynamic Acceleration of the Earth's Rotation", Proc. Roy. Soc. Edinb., 1882.
- [3] Campbell W. H., "Introduction to geomagnetic fields", Cambridge University Press, Cambridge, UK, 1997.
- [4] Lilley, F. E. M., "The Analysis of daily Variations records by Magnetometer Arrays", Geophys. J. R. Astron. Soc., 43, 1-16, 1975.
- [5] Morlet, J., "Sampling Theory and Wave Propagation", Springer, 1983.
- [6] Oczeretko, E., Swiatecka, J., Kitlas, A., Laudanski, T. and Pierzynski, P., "Visualization of synchronization of the uterine contraction signals: Running cross-correlation and wavelet running cross-correlation

- methods”, *Med. Eng. Phys.*, 28, 75-81, 2006.
- [7] Rehman, S. and Siddiqi, A. H., “Wavelet based correlation coefficient of time series of Saudi Meteorological Data”. *Chaos, Solitons and Fractals* 39, 1764–1789, 2009.
- [8] Frick, P., Beck, R., Berkhuijsen, E. M. and Patrickeyev, I., “Scaling and correlation analysis of galactic images”. *Mon. Not. R. Astron. Soc.* 327, 1145–1157, 2001.
- [9] Nesme-Ribes E., Frick P., Sokoloff D., Zakharov V., Ribes J. C., Vigouroux A. and Laclare F. “Wavelet analysis of the Maunder minimum as recorded in solar diameter data”. *C. R. Acad. Sci. Paris*, 321, IIb, 525, 1995.
- [10] Frick P, Baliunas S. L., Galyagin D., Sokoloff D. and Soon W., “Wavelet Analysis of Stellar Chromospheric Activity Variations”, *The Astron. Jour.*, Vol. 483, 426-434, 1997.
- [11] Frick P., Grossmann A. and Tchamitchian P., “Wavelet analysis of signals with gaps”, *Jour. Math. Phys.*, Vol 39, 1998.
- [12] Lindzen R. S. and Chapman S., “Atmospheric tides”, *Sp. Sci. Revs.*, 10, 3-188, 1969.
- [13] Sager, P. Le and Huang T. S., “Longitudinal Dependence of the Daily Geomagnetic Variation during Quiet Time”, *J Geophys. Res.*, A11, 1397, 2002.
- [14] Sizova, L. Z., “The field-aligned currents effect on equatorial geomagnetic field variations”, *Adva. Sp. Res.* 30, 2247 – 2252, 2002.
- [15] Parkinson, W. D., “Introduction to geomagnetism”, *Scottish Acad. Press, Edinburg and London*, 1983.
- [16] Schmucker, U., “A Spherical Harmonic Analysis of Solar Daily Variations in the Years 1964–1965: Response Estimates and Source Fields for Global Induction—I.Methods”, *Geophys. J. Int.*, 136, 439-454, 1999a.
- [17] Schmucker, U., “A Spherical Harmonic Analysis of Solar Daily Variations in the Years 1964–1965: Response Estimates and Source Fields for Global Induction—II. Results”, *Geophys. J. Int.*, 136, 455-476, 1999b.
- [18] Price, A. T., “Daily Variations of the Geomagnetic Field”, *Sp. Sci. Revs.*, 9, 151-197, 1969.
- [19] Wu, C. C., Liou, K., Lepping, R. P., and Meng, C. I., “Identification of substorms within storms”, *Jour. Atmos. Solar-Terr. Phys.* 66 (2), 125-132, 2004.